

# BEHIND THE SCENES: MECHANISTIC INTERPRETABILITY OF LORA-ADAPTED WHISPER FOR SPEECH EMOTION RECOGNITION

Yujian Ma<sup>1,2</sup> Jinqiu Sang<sup>1\*</sup> Ruizhe Li<sup>3</sup>

<sup>1</sup> College of Computer Science and Technology, East China Normal University, Shanghai, China

<sup>2</sup>Shanghai Institute of AI Education, Shanghai, China

<sup>3</sup>Department of Computing Science, University of Aberdeen, Aberdeen, UK

## ABSTRACT

Large pre-trained speech models such as Whisper offer strong generalization but pose significant challenges for resource-efficient adaptation. Low-Rank Adaptation (LoRA) has become a popular parameter-efficient fine-tuning method, yet its underlying mechanisms in speech tasks remain poorly understood. In this work, we conduct the first systematic mechanistic interpretability study of LoRA within the Whisper encoder for speech emotion recognition (SER). Using a suite of analytical tools, including layer contribution probing, logit-lens inspection, and representational similarity via singular value decomposition (SVD) and centered kernel alignment (CKA), we reveal two key mechanisms: a *delayed specialization* process that preserves general features in early layers before consolidating task-specific information, and a *forward alignment, backward differentiation* dynamic between LoRA’s matrices. Our findings clarify how LoRA reshapes encoder hierarchies, providing both empirical insights and a deeper mechanistic understanding for designing efficient and interpretable adaptation strategies in large speech models.

**Index Terms**— Speech Emotion Recognition, Whisper, Mechanistic Interpretability, Low-Rank Adaptation

## 1. INTRODUCTION

Large-scale pre-trained models have fundamentally transformed speech and language processing. Models such as Whisper [1], Wav2Vec2 [2], and HuBERT [3] provide general-purpose representations that are widely adapted to diverse tasks, from automatic speech recognition (ASR) to SER. However, the heavy computational and storage demands of full fine-tuning hinder their deployment in resource-constrained settings. This has motivated the development of Parameter-Efficient Fine-Tuning (PEFT) methods [4, 5], which adapt these large encoders with minimal additional parameters.

Among PEFT approaches, LoRA [6] has demonstrated exceptional effectiveness across modalities including text, vision, and speech [7, 8]. By injecting low-rank trainable matrices into a frozen backbone, LoRA significantly reduces training costs while preserving the model’s powerful representational capacity. Despite its practical success, prior studies primarily emphasize performance gains, leaving a critical question unanswered: why does LoRA work so effectively?

SER serves as a compelling probe for this investigation. Unlike ASR, which primarily relies on lexical content, SER necessitates

capturing subtle prosodic and paralinguistic cues that reflect high-level affective states [9]. This makes SER an ideal testbed for analyzing how LoRA reshapes a model’s internal representations and decision dynamics. Recent work has demonstrated the successful adaptation of both Whisper [10] and Wav2Vec2 [11] for SER, further underscoring the value of exploring parameter-efficient strategies in this domain.

In this work, we present the first systematic mechanistic analysis of LoRA within the Whisper encoder for SER. We employ a multi-faceted interpretability toolkit that includes layer-wise contribution probing [12], Logit-Lens inspection [13], and representation analyses with SVD and CKA [14]. Our findings reveal two key mechanisms underlying LoRA’s success: a depth-specific *delayed specialization* strategy and a *forward alignment, backward differentiation* dynamic between LoRA’s low-rank matrices. These insights clarify how LoRA reorganizes encoder hierarchies and provide a foundation for designing more efficient and interpretable fine-tuning strategies for deep speech models.

## 2. RELATED WORK

### 2.1. Mechanistic Interpretability

Mechanistic interpretability (MI) is an emerging field that seeks to reverse-engineer the internal computations of deep networks to understand the algorithms they have learned [15]. In the domain of natural language processing (NLP), MI studies have shed light on how large language models (LLMs) encode complex behaviors like arithmetic and reasoning [16, 17]. For instance, Csordás et al. investigated the efficient use of network depth, revealing that in deep LLMs, the latter half of the network is often underutilized, primarily refining the output probability distribution rather than performing novel computations [12]. Building on this analytical framework, the ‘Backward Lens’ study extended it to the backward pass, revealing a two-phase ‘imprint and shift’ mechanism for how models store new knowledge in their feed-forward layers [18]. Recent multimodal efforts, such as AudioLens [19], have further applied these principles to understand auditory perception in large audio-language models. However, within the speech processing community, MI remains limited, with most work focusing on probing intermediate representations rather than the intricate adaptation mechanisms of fine-tuning strategies like LoRA.

### 2.2. Speech Emotion Recognition

SER has evolved significantly, progressing from systems based on hand-crafted features [20] to those leveraging powerful self-supervised encoders like Wav2Vec2 [2] and HuBERT [3], and

\*Corresponding author.

more recently, large pre-trained models such as Whisper [1]. This evolution has led to notable improvements in cross-speaker and cross-domain robustness [9]. Task-specific fine-tuning approaches, including those that incorporate metadata-enhanced strategies [21] and domain generalization for Whisper [10], have shown promising results. Nevertheless, the substantial computational and storage costs associated with full fine-tuning necessitate the exploration of more resource-efficient alternatives [22].

### 2.3. Parameter-Efficient Fine-Tuning

Parameter-Efficient Fine-Tuning methods [4, 5] offer a compelling solution by adapting frozen backbones with a minimal number of trainable parameters. Popular approaches include adapters, prefix-tuning, and prompt-tuning, among which LoRA [6] has demonstrated exceptional effectiveness. While adapters may introduce inference latency and prefix-tuning can be unstable for speech tasks, LoRA achieves remarkable efficiency without sacrificing performance by injecting low-rank updates. Its efficacy has been confirmed in various applications, including Whisper for ASR [8], yet the precise inner adaptation dynamics of LoRA for complex tasks like SER remain largely unexplored.

### 2.4. Research Gap

In summary, existing literature has made significant strides in three distinct areas: mechanistic interpretability in NLP, the application of large pretrained encoders for SER, and the development of PEFT methods for speech. However, the intersection of these fields, specifically the mechanistic interpretability of LoRA’s adaptation in speech emotion recognition, has not been systematically investigated. This work is dedicated to bridging this critical research gap by analyzing how LoRA reshapes the representational hierarchies and optimization dynamics within the Whisper encoder for the SER task.

## 3. EXPERIMENTAL SETUP

SER is formulated as a four-class task (*anger, happiness, neutrality, sadness*) with WhisperForAudioClassification as the backbone. We conduct experiments on the IEMOCAP [23] dataset using a speaker-independent 10-fold cross-validation. Unweighted recall (UAR) and weighted recall (WAR) serve as our evaluation metrics; UAR provides a robust measure for imbalanced datasets, while WAR reflects overall accuracy. For our mechanistic analysis, we use the Whisper-large-v2 encoder and the NNsight [24] library, with analysis based on a hierarchical sample of 100 examples from a validation set (25 from each emotion class).

### 3.1. LoRA Fine-tuning

We adopt LoRA as our primary fine-tuning method, which approximates weight updates via a low-rank decomposition,  $\Delta W = BA$ . Only the low-rank matrices  $A \in \mathbb{R}^{r \times d}$  and  $B \in \mathbb{R}^{d \times r}$  are trainable, significantly reducing the number of parameters. We attach LoRA modules to the attention projections, a standard and effective strategy. Unless otherwise noted, we use a configuration of  $r=32$  and apply a dropout of 0.1, with a trainable classification head.

As shown in Table 1, LoRA consistently and significantly outperforms the frozen-encoder baselines across all model sizes. The Whisper-large-v2 with LoRA achieves the best performance, with

**Table 1.** SER performance on IEMOCAP under speaker-independent 10-fold cross-validation. Results are mean  $\pm$  std.

Model	LoRA		Frozen-Encoder	
	UAR	WAR	UAR	WAR
tiny	0.670 $\pm$ 0.026	0.664 $\pm$ 0.028	0.485 $\pm$ 0.033	0.502 $\pm$ 0.028
base	0.702 $\pm$ 0.025	0.692 $\pm$ 0.025	0.517 $\pm$ 0.036	0.530 $\pm$ 0.029
small	0.728 $\pm$ 0.034	0.723 $\pm$ 0.036	0.545 $\pm$ 0.036	0.558 $\pm$ 0.036
medium	0.758 $\pm$ 0.030	0.756 $\pm$ 0.031	0.638 $\pm$ 0.037	0.641 $\pm$ 0.032
large-v2	<b>0.774 <math>\pm</math> 0.026</b>	<b>0.768 <math>\pm</math> 0.035</b>	0.582 $\pm$ 0.044	0.588 $\pm$ 0.041
large-v3	0.767 $\pm$ 0.034	0.763 $\pm$ 0.036	0.433 $\pm$ 0.031	0.459 $\pm$ 0.036

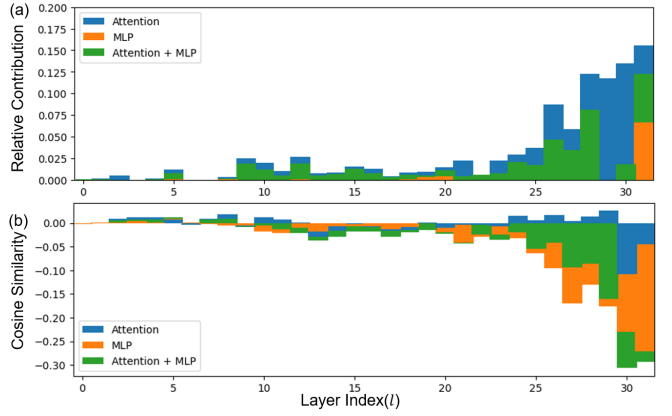


**Fig. 1.** Layer-wise differences (LoRA minus frozen) on the encoder residual stream: (a) mean relative contribution and (b) cosine similarity for self-attention, MLP, and their sum.

a UAR of 0.774 and WAR of 0.768, demonstrating substantial improvements over its frozen counterpart. The performance of LoRA scales consistently with model size, highlighting its ability to effectively leverage larger pre-trained representations. In stark contrast, the frozen-encoder results show irregular patterns, which may reflect a fundamental incompatibility between the model’s original ASR representations and the demands of the SER task. Our subsequent mechanistic analysis aims to clarify how LoRA effectively resolves this representational conflict.

### 3.2. Layer Contribution Probing

Our analysis of layer-wise contributions is conceptually inspired by recent work on analyzing the depth efficiency of language models [12]. We extend this methodology to the LoRA-adapted Whisper encoder by decomposing each Transformer block into its self-attention and MLP sublayers and measuring their effects on the residual stream. For a given layer  $\ell$  with residual state  $\mathbf{h}_\ell$ , attention output  $\mathbf{a}_\ell$ , and MLP output  $\mathbf{m}_\ell$ , we compute the relative contribution ratios  $\|\mathbf{a}_\ell\|_2/\|\mathbf{h}_\ell\|_2$  and  $\|\mathbf{m}_\ell\|_2/\|\mathbf{h}_\ell\|_2$ . We also measure the directional alignment of these outputs with the residual stream using cosine similarity:  $\cos(\mathbf{a}_\ell, \mathbf{h}_\ell)$  and  $\cos(\mathbf{m}_\ell, \mathbf{h}_\ell)$ . To isolate LoRA’s specific effect, we report the per-layer differences  $\Delta = (LoRA - frozen)$  averaged over the evaluation data, as shown in Fig. 1.

While LoRA introduces negligible changes in the early layers, its relative contribution increases substantially towards the top of the encoder, indicating a depth-specific adaptation strategy. In these deeper layers, the attention sublayer’s contribution grows more than

the MLP’s, suggesting a primary role for LoRA in sharpening temporal focusing and long-range integration. This effect is further complemented by the combined Attention+MLP curve in the top layers, which evidences a synergistic interplay by exceeding the contribution of either component alone. The increasingly negative cosine similarity at higher layers indicates that the updates introduced by LoRA, which are directly applied to the Attention layers, are progressively passed to the subsequent layers. This suggests that the model’s self-attention mechanism, having been finely tuned by LoRA to focus on emotional features, actively introduces signals that are counter-directional to the residual stream’s information flow in the MLP layers. This is a critical mechanism for effective fine-tuning: by introducing these “subtractive” or “corrective” signals, LoRA is able to suppress or filter out features from the frozen backbone that are irrelevant or distracting to the new SER task. This targeted suppression allows the model to re-allocate its representational capacity, thereby emphasizing and reinforcing the task-relevant emotional features for a more robust and decisive final prediction.

### 3.3. Logit-Lens Inspection

To understand how discriminative information propagates through the encoder hierarchy, we conduct a Logit-Lens analysis [13]. The core idea of this method is to inspect the “mind” of the model by projecting the intermediate representations of each layer directly to the final output space. This allows us to observe the layer-wise evolution of the model’s predictions. For each layer  $\ell$ , we extract the representation  $\mathbf{h}_\ell$ , then apply the trained projector and classifier to obtain intermediate logits  $\mathbf{z}_\ell = \text{Classifier}(\text{Project}(\mathbf{h}_\ell))$ .

We quantify the alignment between intermediate and final predictions using two complementary metrics:

1. **KL Divergence:**  $D_{KL}(\pi_\ell \| \pi_L) = \sum_c \pi_\ell(c) \log \frac{\pi_\ell(c)}{\pi_L(c)}$ , where  $\pi_\ell = \text{softmax}(\mathbf{z}_\ell)$  and  $\pi_L$  is the final prediction. Lower values indicate better alignment.
2. **Prediction Overlap:**  $O_\ell = \mathbb{I}[\arg \max(\mathbf{z}_\ell) = \arg \max(\mathbf{z}_L)]$ , measuring whether intermediate and final predictions agree. Higher values indicate stronger consistency.

As shown in Figure 2a, the two models exhibit distinct depth-wise alignment patterns. The frozen encoder shows volatile KL curves in early layers, drops to a minimum near layer 27, then rebounds at the top. This suggests that while Whisper possesses latent emotion-related capacity, achieving strongest emotional expression at the KL minimum, the original ASR objective creates inherent instability requiring downstream classifier compensation.

In contrast, the LoRA-adapted encoder employs a “delayed decision-making” strategy that maintains a relatively flat and high KL across the early and middle layers, then undergoes a pronounced late-stage drop converging to a very low value at the top. Rather than producing the chaotic signals observed in the frozen encoder, LoRA preserves a “stable yet unspecialized” state in the early layers, laying a smooth foundation for final specialization. This strategy allows LoRA to avoid premature commitment to task-specific representations while ensuring that the eventual specialization is both decisive and robust. This observation corroborates our findings in Section 3.2, as both the Logit-Lens and Layer Contribution analyses converge on a shared conclusion: LoRA’s most significant contributions are concentrated in the deeper layers of the encoder.

The prediction-overlap curves further corroborate this delayed specialization mechanism. The frozen encoder begins to increase

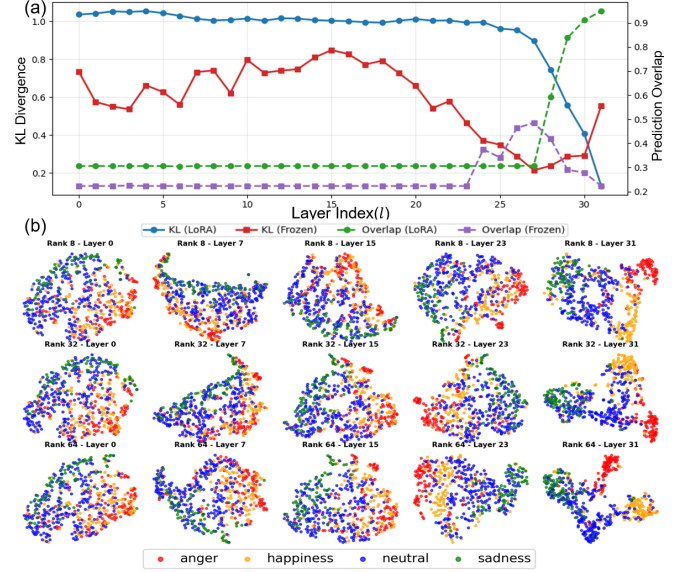


**Fig. 2.** Layer-wise analysis of LoRA’s internal representations. (a) Logit-Lens analysis. (b) t-SNE visualization across different LoRA ranks.

overlap earlier (around layer 23) but subsequently declines, mirroring the instability seen in its KL trajectory. The LoRA-adapted encoder maintains a higher and steady overlap up to the mid-upper layers, then shows a sharp rise starting around layer 27, quickly approaching near-perfect agreement at the top. This delayed but decisive top-1 prediction consolidation demonstrates LoRA’s ability to defer critical decisions until the optimal moment, when sufficient task-relevant information has been accumulated and refined.

Taken together, these trends reveal that LoRA fundamentally restructures the information flow within the encoder: rather than relying on the original model’s unstable emotional representations, it establishes a controlled, late-stage specialization process that preserves general representations in earlier layers while performing targeted, robust specialization where it is most effective. This controlled, late-stage specialization process not only improves performance but also enhances the stability and interpretability of the model’s decision-making process.

### 3.4. Rank-Based Representation Analysis

Our t-SNE analysis across different LoRA ranks ( $r = 8, 32, 64$ ) reveals a systematic improvement in emotion clustering quality with increasing rank capacity. As shown in Figure 2b, deeper layers with  $r = 64$  achieve the most distinct and well-separated emotion boundaries, while maintaining a consistent depth-wise evolution from mixed to specialized representations. This pattern reinforces our delayed decision-making hypothesis: while the fundamental specialization mechanism remains consistent across ranks, LoRA’s representational capacity directly determines the final clustering quality and emotion separability. Low-rank configurations ( $r = 8$ ) demonstrate a fundamental limitation, exhibiting persistent inter-class overlap even in the deepest layers, suggesting minimal rank capacity constrains the model’s ability to achieve complete emotion separation.

An emotion-specific analysis reveals a hierarchy of rank-sensitivity. Neutral emotions maintain stable clustering across all

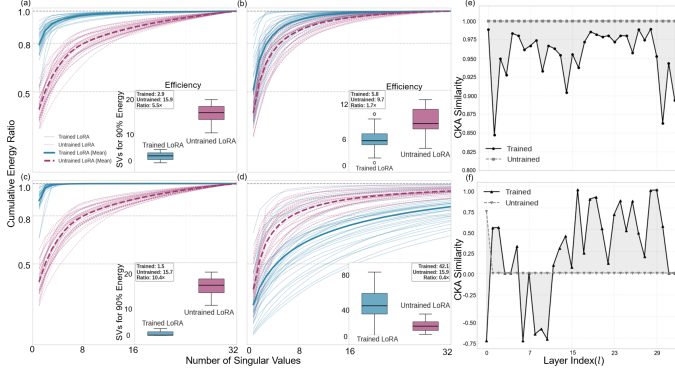


**Fig. 3.** Analysis of LoRA’s internal dynamics. (a)-(d): SVD analysis. (a, c) are for LoRA<sub>A</sub> and LoRA<sub>B</sub> activations, while (b, d) are for their gradients. (e), (f): CKA similarity for activations and gradients.

ranks, likely due to their high frequency in the original Whisper training data. Sadness shows moderate rank-sensitivity, forming coherent clusters at  $r = 32$  and above, but fragmenting at  $r = 8$ . In contrast, anger and happiness require higher representational capacity ( $r = 64$ ) for clear separation, with  $r = 8$  configurations showing severe confusion. This hierarchy—neutral < sadness < anger < happiness—suggests that the recognition of positive emotions demands the highest level of LoRA sophistication, likely due to their nuanced acoustic expressions and the need for fine-grained feature discrimination.

### 3.5. Singular Value Decomposition Analysis

To investigate the intrinsic dimensionality and learning dynamics of LoRA, we conduct a comprehensive SVD analysis on its low-rank matrices across all layers. The “LoRA (mean)” is computed by averaging the singular values from all attention heads and all layers, providing a global perspective on its learning dynamics. By comparing a trained LoRA model against a randomly initialized counterpart, we analyze how each component concentrates energy within its dominant singular values. This analysis reveals a sophisticated division of labor between LoRA’s matrices, which develop specialized, complementary roles for compression and reconstruction.

The LoRA<sub>A</sub> matrix functions as an adaptive compression encoder, projecting high-dimensional input representations into task-relevant low-dimensional subspaces. As shown in its activation spectrum (Figure 3a), the trained LoRA<sub>A</sub> exhibits dramatic compression efficiency, requiring only 2.9 singular values to capture 90% of the energy—a remarkable 5.5 $\times$  improvement over the untrained baseline. This efficiency is also reflected in its gradient spectrum (Figure 3b), which shows a 1.7 $\times$  improvement in concentration, indicating that the training process focuses on identifying optimal directions for feature compression.

Conversely, the LoRA<sub>B</sub> matrix operates as a precision reconstructor. Its post-training activation spectrum (Figure 3c) demonstrates even more extreme compression efficiency, with a 10.4 $\times$  improvement over the untrained model. However, a crucial asymmetry emerges in its gradient dynamics: the trained LoRA<sub>B</sub> (Figure 3d) exhibits higher dimensionality than its untrained counterpart, representing a 0.4 $\times$  efficiency ratio. This counterintuitive pattern reveals that while LoRA<sub>B</sub> produces highly compressed forward activations, it deliberately maintains rich gradient diversity during the backward

pass to enable fine-grained reconstruction control.

This complementary learning architecture—where LoRA<sub>A</sub> acts as an information compressor and LoRA<sub>B</sub> as a precision reconstructor—is a key to LoRA’s exceptional efficiency. This synergistic specialization ensures both aggressive forward compression and preserved gradient dimensionality, validating that LoRA operates within the intrinsic low-dimensional manifold of the adaptation task.

### 3.6. Centered Kernel Alignment Analysis

To quantify the representational similarity between LoRA components, we employ CKA. Unlike simple metrics such as cosine similarity, CKA provides a robust, normalized score invariant to linear transformations, making it ideal for comparing neural network representations. High values suggest the components capture similar representational structures, while low or negative values indicate dissimilar or inversely related structures

$$\text{CKA}(\mathbf{X}, \mathbf{Y}) = \frac{\text{HSIC}(\mathbf{K}, \mathbf{L})}{\sqrt{\text{HSIC}(\mathbf{K}, \mathbf{K}) \cdot \text{HSIC}(\mathbf{L}, \mathbf{L})}} \quad (1)$$

where  $\mathbf{K}$  and  $\mathbf{L}$  are kernel matrices derived from representations  $\mathbf{X}$  and  $\mathbf{Y}$ , and HSIC is the Hilbert-Schmidt Independence Criterion.

As depicted in Figure 3ef, our analysis reveals a crucial asymmetry in LoRA’s learning dynamics. The forward passes of the LoRA components consistently maintain high representational similarity (0.8-1.0), indicating that LoRA’s forward pass acts as a coherent information flow. In stark contrast, their corresponding gradient similarities exhibit a substantial variability, ranging from high positive to negative correlations. The presence of negative correlations is particularly revealing, as it indicates an antagonistic optimization dynamic, where LoRA<sub>A</sub> and LoRA<sub>B</sub> actively pull in opposite directions in certain layers during the backward pass.

This finding elucidates a fundamental forward alignment, backward differentiation mechanism. It shows that LoRA achieves representational consistency during inference (forward) while maintaining specialized, fine-grained optimization roles during training (backward). Our analysis suggests that LoRA<sub>A</sub> functions primarily as a feature compressor, guided by these differentiated backward signals, while LoRA<sub>B</sub> acts as a precision reconstructor. This synergistic specialization enables LoRA to achieve exceptional parameter efficiency without sacrificing the model’s overall expressivity.

## 4. CONCLUSION

This paper presents the first systematic mechanistic analysis of LoRA in the Whisper encoder for SER. Our analysis reveals two key mechanisms for its superior performance: “delayed specialization”, which preserves stable representations in early layers for decisive late-stage consolidation, and a “forward alignment, backward differentiation” dynamic between LoRA’s matrices. These insights not only clarify LoRA’s effectiveness but also establish a theoretical foundation for understanding low-rank fine-tuning in deep speech models. By demonstrating how a small number of parameters can fundamentally restructure the information flow, our work paves the way for the design of more efficient and interpretable adaptation strategies. Future work will investigate whether these dynamics generalize to other speech tasks, such as multilingual emotion recognition or speaker identification, and whether they are consistent across different large-scale pre-trained models.

## 5. ACKNOWLEDGEMENTS

This work was supported by the National Natural Science Foundation of China (Grant No. 12411530075) and the Royal Society (Grant No. IEC\NSFC\233558).

## 6. REFERENCES

- [1] Alec Radford, Jong Wook Kim, Tao Xu, Greg Brockman, Christine McLeavey, and Ilya Sutskever, “Robust speech recognition via large-scale weak supervision,” in *International conference on machine learning*. PMLR, 2023, pp. 28492–28518.
- [2] Alexei Baevski, Yuhao Zhou, Abdelrahman Mohamed, and Michael Auli, “wav2vec 2.0: A framework for self-supervised learning of speech representations,” *Advances in neural information processing systems*, vol. 33, pp. 12449–12460, 2020.
- [3] Wei-Ning Hsu, Benjamin Bolte, Yao-Hung Hubert Tsai, Kushal Lakhotia, Ruslan Salakhutdinov, and Abdelrahman Mohamed, “Hubert: Self-supervised speech representation learning by masked prediction of hidden units,” *IEEE/ACM transactions on audio, speech, and language processing*, vol. 29, pp. 3451–3460, 2021.
- [4] Luping Wang, Sheng Chen, Linnan Jiang, Shu Pan, Runze Cai, Sen Yang, and Fei Yang, “Parameter-efficient fine-tuning in large language models: a survey of methodologies,” *Artificial Intelligence Review*, vol. 58, no. 8, pp. 227, 2025.
- [5] Nakamasa Inoue, Shinta Otake, Takumi Hirose, Masanari Ohi, and Rei Kawakami, “Elp-adapters: Parameter efficient adapter tuning for various speech processing tasks,” *IEEE/ACM Transactions on Audio, Speech, and Language Processing*, 2024.
- [6] Edward J Hu, Yelong Shen, Phillip Wallis, Zeyuan Allen-Zhu, Yuanzhi Li, Shean Wang, Lu Wang, Weizhu Chen, et al., “Lora: Low-rank adaptation of large language models..,” *ICLR*, vol. 1, no. 2, pp. 3, 2022.
- [7] Rizhao Cai, Zitong Yu, Chenqi Kong, Haoliang Li, Changsheng Chen, Yongjian Hu, and Alex C Kot, “S-adapter: Generalizing vision transformer for face anti-spoofing with statistical tokens,” *IEEE Transactions on Information Forensics and Security*, vol. 19, pp. 8385–8397, 2024.
- [8] Zheshu Song, Jianheng Zhuo, Yifan Yang, Ziyang Ma, Shixiong Zhang, and Xie Chen, “Lora-whisper: Parameter-efficient and extensible multilingual asr,” *arXiv preprint arXiv:2406.06619*, 2024.
- [9] Siddique Latif, Rajib Rana, Sara Khalifa, Raja Jurdak, Junaid Qadir, and Björn Schuller, “Survey of deep representation learning for speech emotion recognition,” *IEEE Transactions on Affective Computing*, vol. 14, no. 2, pp. 1634–1654, 2021.
- [10] Erik Goron, Lena Asai, Elias Rut, and Martin Dinov, “Improving domain generalization in speech emotion recognition with whisper,” in *ICASSP 2024-2024 IEEE International Conference on Acoustics, Speech and Signal Processing (ICASSP)*. IEEE, 2024, pp. 11631–11635.
- [11] Li-Wei Chen and Alexander Rudnicky, “Exploring wav2vec 2.0 fine tuning for improved speech emotion recognition,” in *ICASSP 2023-2023 IEEE international conference on acoustics, speech and signal processing (ICASSP)*. IEEE, 2023, pp. 1–5.
- [12] Róbert Csordás, Christopher D Manning, and Christopher Potts, “Do language models use their depth efficiently?,” *arXiv preprint arXiv:2505.13898*, 2025.
- [13] Nostalggebraist, “Interpreting gpt: the logit lens,” <https://www.lesswrong.com/posts/AcKRB8wDpdaN6v6ru/interpreting-gpt-the-logit-lens>, August 2020.
- [14] Simon Kornblith, Mohammad Norouzi, Honglak Lee, and Geoffrey Hinton, “Similarity of neural network representations revisited,” in *International conference on machine learning*. PMIR, 2019, pp. 3519–3529.
- [15] Daking Rai, Yilun Zhou, Shi Feng, Abulhair Saparov, and Ziyu Yao, “A practical review of mechanistic interpretability for transformer-based language models,” *arXiv preprint arXiv:2407.02646*, 2024.
- [16] Ruizhe Li and Yanjun Gao, “Anchored answers: Unravelling positional bias in gpt-2’s multiple-choice questions,” *arXiv preprint arXiv:2405.03205*, 2024.
- [17] Ruizhe Li, Chen Chen, Yuchen Hu, Yanjun Gao, Xi Wang, and Emine Yilmaz, “Attributing response to context: A jensen-shannon divergence driven mechanistic study of context attribution in retrieval-augmented generation,” *arXiv preprint arXiv:2505.16415*, 2025.
- [18] Shahar Katz, Yonatan Belinkov, Mor Geva, and Lior Wolf, “Backward lens: Projecting language model gradients into the vocabulary space,” *arXiv preprint arXiv:2402.12865*, 2024.
- [19] Chih-Kai Yang, Neo Ho, Yi-Jyun Lee, and Hung-yi Lee, “Audiolens: A closer look at auditory attribute perception of large audio-language models,” *arXiv preprint arXiv:2506.05140*, 2025.
- [20] Björn Schuller, Gerhard Rigoll, and Manfred Lang, “Speech emotion recognition combining acoustic features and linguistic information in a hybrid support vector machine-belief network architecture,” in *2004 IEEE international conference on acoustics, speech, and signal processing*. IEEE, 2004, vol. 1, pp. I–577.
- [21] Zixiang Wan, Ziyue Qiu, Yiyang Liu, and Wei-Qiang Zhang, “Metadata-enhanced speech emotion recognition: Augmented residual integration and co-attention in two-stage fine-tuning,” in *ICASSP 2025-2025 IEEE International Conference on Acoustics, Speech and Signal Processing (ICASSP)*. IEEE, 2025, pp. 1–5.
- [22] Nineli Lashkarashvili, Wen Wu, Guangzhi Sun, and Philip C Woodland, “Parameter efficient finetuning for speech emotion recognition and domain adaptation,” in *ICASSP 2024-2024 IEEE International Conference on Acoustics, Speech and Signal Processing (ICASSP)*. IEEE, 2024, pp. 10986–10990.
- [23] Carlos Busso, Murtaza Bulut, Chi-Chun Lee, Abe Kazemzadeh, Emily Mower, Samuel Kim, Jeannette N Chang, Sungbok Lee, and Shrikanth S Narayanan, “Iemocap: Interactive emotional dyadic motion capture database,” *Language resources and evaluation*, vol. 42, no. 4, pp. 335–359, 2008.
- [24] Jaden Fiotto-Kaufman, Alexander R Loftus, Eric Todd, Jan-nik Brinkmann, Koyena Pal, Dmitrii Troitskii, Michael Ripa, Adam Belfki, Can Rager, Caden Juang, et al., “Nnsight and ndif: Democratizing access to open-weight foundation model internals,” *arXiv preprint arXiv:2407.14561*, 2024.